

# Parametric Study of Gas Tungsten Arc Welding on Mechanical Properties of Low Carbon Steel

Vijander Kumar

Assistant Professor

Sant Longowal Institute of Engineering & Technology, Longowal - 148106, Punjab, India

**Abstract**— In the present research work an attempt is made to understand the effect of TIG welding parameters such as welding current, gas flow rate, welding speed, weld torch angle that are influences on responsive output parameters such as weld penetration, width, fusion area, micro hardness, and tensile strength of welding. Taguchi method is used to get the optimal parameters. In Taguchi method, L9 orthogonal array is used for experimentation. The effort made to investigate optimal machining parameters and their contribution for producing better weld quality and higher Productivity. After welding test for weld penetration, weld width, fusion area, tensile test, and micro hardness have been conducted. The significance of the factors on overall output feature of the weldment has also been evaluated by analysis of variance (ANOVA).

**Key words:** GTAW, Hardness, Tensile Strength, Weld Geometry

## I. INTRODUCTION

The use of TIG today has spread to a variety of metals like stainless mild and high tensile steels. GTAW is most commonly called TIG (Tungsten Inert Gas).

Electrode used in GTAW is non consumable tungsten and maximum thickness of plate which can be joined by GTAW is less due to low penetration. Enhancement in weld geometry has long been sought in Gas Tungsten Arc Welding. DCSP - Direct Current Straight Polarity DCRP - Direct Current Reverse Polarity AC Alternating Current can be used for TIG. Out of these alternating current is the preferred welding current for most white metals, eg aluminum and magnesium. Some researcher work for the selection of process parameters to obtained an optimal weld pool geometry in the tungsten inert gas (TIG) welding of stainless steel was presented.[6] It may be conclude that Heat affected zone decreases the strength of the weld[1] Investigated high cycle and low cycle fatigue properties of SUS304L, SUS316L steel and the effects of welding structure by GTAW welding process[25].The job of the shielding gas is to protect the weld pool contamination from air, The most dominant mechanism for increased penetration was considered to be arc constriction rather than a change in the surface tension of the molten pool.[7] . Weld torch angle have highly influence on the heat which are supply to work piece the non-consumable electrode angle influences the weld penetration depth and the weld shape The most plausible mechanism at present is that the arc or plasma was constricted by the action of the A-TIG fluxes and that the associated increase in current density results in increased forces which alter the molten pool flow to give higher penetration From literature study it can be conclude that Higher current in TIG welding can lead to splatter and work piece become damage. Again lower current setting in TIG welding lead to sticking of the filler wire.

Sometimes larger heat affected area can be found for lower welding current, as high temperatures need to applied for longer periods of time to deposit the same amount of filling materials The choice of shielding gas is depends on the working metals and effects on the welding cost, weld temperature, arc stability, weld speed, splatter, electrode life etc Argon or Helium may be used successfully for TIG welding applications. For welding of extremely thin material pure argon is used. Excessive high welding speed decreases wetting action, increases tendency of undercut, porosity and uneven bead shapes while slower welding speed reduces the tendency to porosity.

The TIG welding process enjoys widespread use because of its ability to provide high quality welds with high production rate, for a wide range of ferrous and non-ferrous alloys.

## II. MATERIALS AND METHODS

The chemical composition of Low carbon alloy steel is used Is shown in Table 2.1

C	Si	S	Mn	P	C equi.
0.23	0.4	0.045	1.5	.045	0.42

Table 1: Chemical Composition of Base Metal

Specimen size 200mm x 75mm x 5mm were cut from the plate which were roughly polished with 400 grit abrasive paper to remove surface impurities and then washed with acetone. Welding is done in a single pass. The input parameter were selected on the basis of a series of pilot experiments combined with the data obtained from the literature review As a result input parameter were selected as shown in Table 2.2

Input Parameter	Levels
Current (Ampere)	110-130-150
Torch Travel Speed (Mm/S)	1-1.75-2.50
Gas Flow Rate (Lit/Minute)	10-12-14
Torch Angle (Degree)	60-75-90

Table 2: Input Parameters and Their Levels

The experimental layout for the parameter, using the L<sub>9</sub> (3<sup>3</sup>) orthogonal arrays is shown in Table 2.3

Sr. No	Current (Ampere)	Weld speed (m/min)	Gas flow rate (lit/min)	Torch angle (Degree)
1	110	1	10	60
2	110	1.75	12	75
3	110	2.5	14	90
4	130	1	12	90
5	130	1.75	14	60
6	130	2.5	10	75
7	150	1	14	75
8	150	1.75	10	90
9	150	2.5	12	60

Table 3: Levels of Process Parameters used in Taguchi L9

A. Orthogonal Array

After welding was done on the samples, the raw welded samples were cut using the power hack-saw machine for checking the tensile strength. Smaller piece for micro hardness and weld geometry were cut by using the Meta cut abrasive cutting machine. After welding, the cross-sections of the welded seams were prepared by standard metallographic procedures, such as sectioning, polishing and etching. In sectioning, samples were cut into size of 50x20mm from welded pieces to measure weld bead profile and 150mmx25mm for tensile strength. Now polishing was done such that one by one all emery papers of grade 160, 220, 320, 400, 600, 800, 1000 and 1200 were used in ascending order on every sample as given in above list. After using abrasive paper, Velvet Cloth, Alumina Powder and Diamond Paste 5µ also used for getting reflecting surface, after using diamond paste, specimen are ready for etching operation. Etching is done to highlight the weld bead and identify microstructure feature or phases present. For detecting the weld bead border we need etching with a proper solution that attacks the metal in such a way that the specific features are made to stand out.

For etching operation require chemical mixture of HCL and HNO<sub>3</sub> in equal pro-portion of 10 ml. specimen was dipped into the etchant for two minutes. The exothermic reaction takes place results in revealing the weld bead of the sample. The sample was immediately washed under running water and dried with air blower. After proper etching of the specimen, the weld bead will be visible. After that getting it dried by air blower all specimen are scanned with the help of scanner. These scanned images are measured for bead height, bead width and depth of penetration with the help of Adobe Acrobat Professional 11 software. These dimensions of response are analyzed in design expert 7.0.0 software.

III. RESULTS AND DISCUSSION

Etched samples were analysis for weld geometry and micro hardness. Tensile test was conducted separately.

A. Analysis and Result for Weld Geometry

Three sets of test were performed and average value was taken. Result for weld geometry is shown in Table 3.1

Sr. No.	Penetration (mm)	Width (mm)	Area (mm <sup>2</sup> )
1	2.98	4.2	9.13
2	2.21	3.9	8.14
3	1.80	2.94	3.84
4	3.50	6.86	13.97
5	2.80	4.48	10.48
6	1.32	5.20	5.00
7	4.56	6.88	18.76
8	3.09	7.78	12.91
9	1.88	4.70	7.81

Table 4: Dimension of Weld Geometry

It was found that maximum penetration was 4.56 mm for sample number operated on 150 ampere current, 1 m/min weld speed 14 lit/min gas flow rate and 75 degree torch angle and minimum weld width and weld area were for sample number operated on 110 ampere current 2.5 m/min weld speed 14 lit/min gas flow rate and 90 degree torch angle.

B. Analysis and Result for Tensile Strength

Tensile test of the welded joint was performed with universal tensile testing machine with maximum load capacity 600 kN.

Sample No.	Load (kN)	Ultimate Tensile Strength (Mpa)
1	66.45	265.8
2	50.32	201.3
3	40.78	163.1
4	81.6	326.4
5	58.7	234.8
6	35.7	142.8
7	88.9	355.6
8	67.4	269.8
9	40.8	163.2

Table 5: Experimental result for tensile strength

Table 3.2 shows the tensile strength value for all the welded joints produced at different welding speed and current setting. It was found that maximum tensile strength was 355.6 Mpa which is lower than the tensile strength of the parent metal UTS of 448 Mpa for sample operated on 150 ampere current, 1 m/min weld speed 14 lit/min gas flow rate and 75 degree torch.

C. Analysis and Result for Micro Hardness

Micro hardness test were performed on Vicker hardness machine which generated diamond shape indentation. Seven readings of each piece one at the mid of weld bead, three in left hand side and three in right hand from the mid of weld bead were taken. The result were shown graphically for each work piece separately.

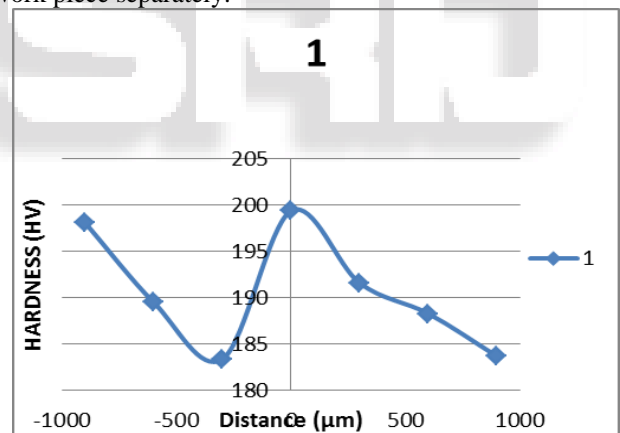


Fig. 1: Hardness Graph For Sample No -1

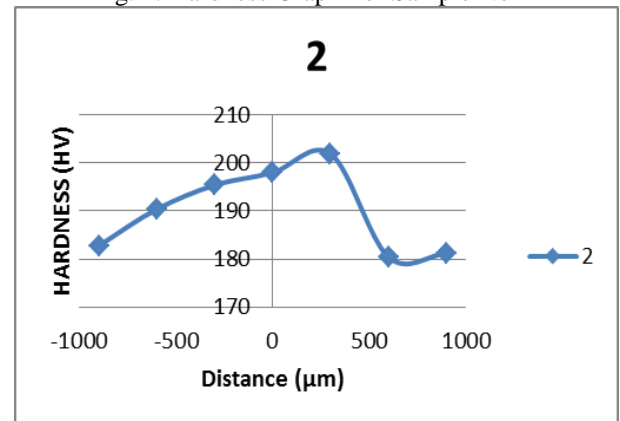


Fig. 2: Hardness Graph For Sample No -1

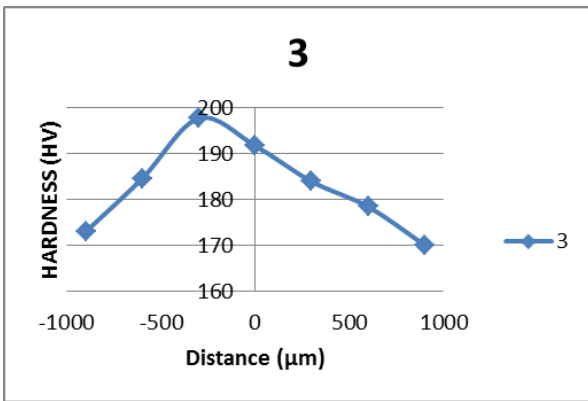


Fig. 3: Hardness Graph For Sample No -1

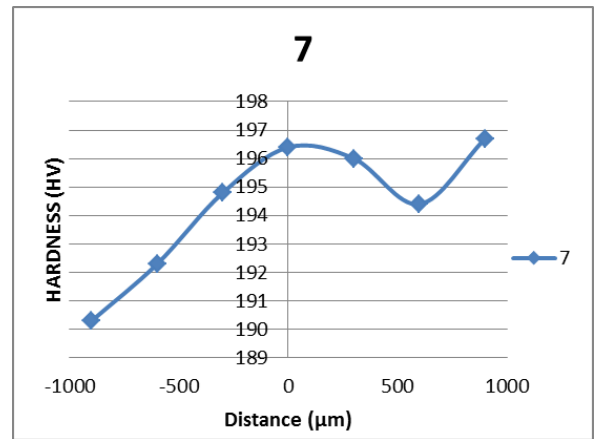


Fig. 6: Hardness Graph For Sample No -1

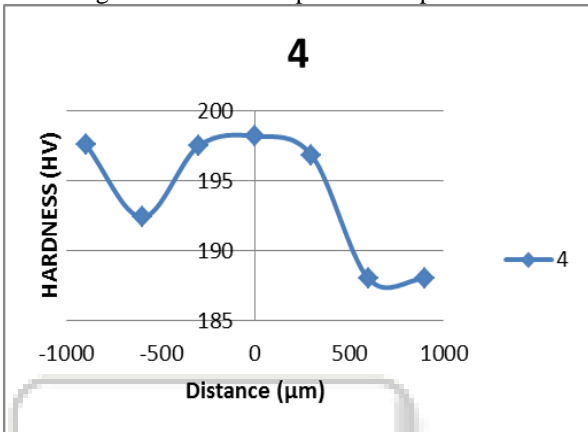


Fig. 4: Hardness Graph For Sample No -1

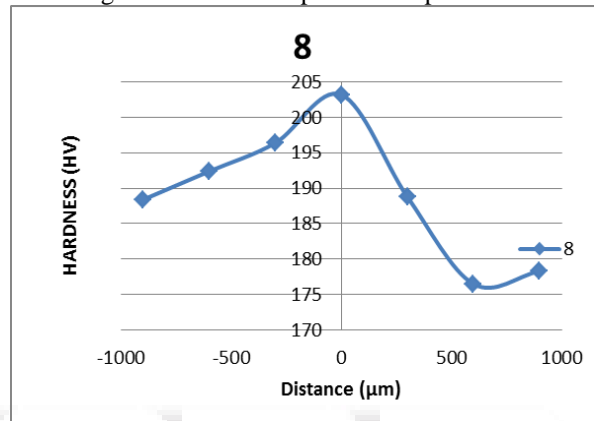


Fig. 7: Hardness Graph For Sample No -1

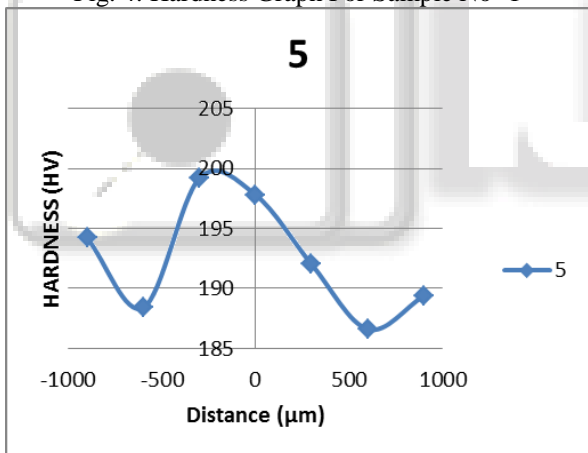


Fig. 5: Hardness Graph For Sample No -1

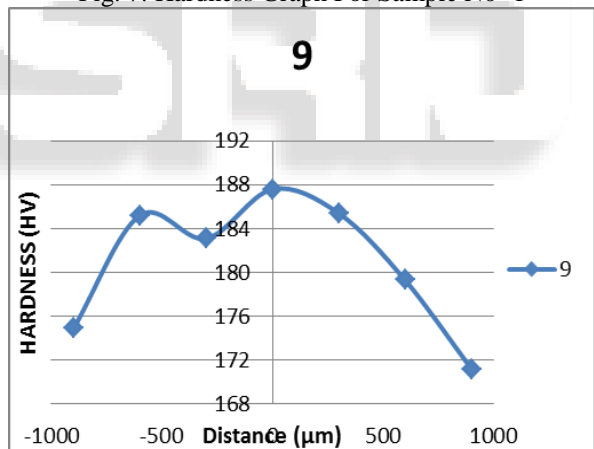


Fig. 8: Hardness Graph For Sample No -1

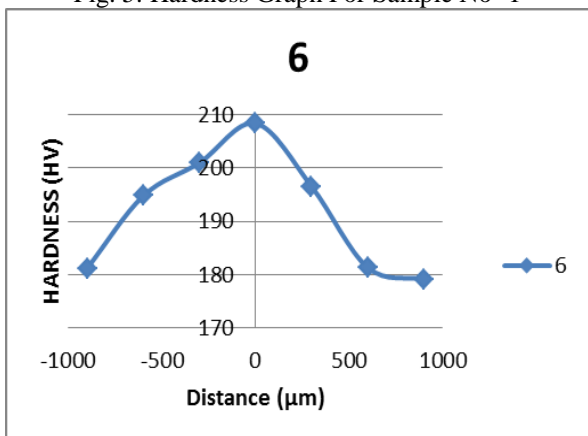


Fig. 5: Hardness Graph For Sample No -1

#### IV. CONCLUSION OF THE PRESENT STUDY

- 1) Visual inspection shows some defects like little undercut at the end, and lack of penetration in few samples. However, under certain combinations of current, weld speed, gas flow rate and torch angle, the joints were found defect free.
- 2) From the tensile test of the samples, it was observed that ultimate tensile strength is satisfactory for many of the joints made at different levels of current, weld speed, gas flow rate and torch angle.
- 3) From the micro-hardness tests it was observed that the hardness value increased from base region to HAZ and HAZ to weld region. However, consistency in this trend is not observed for all the samples.

- 4) Surface plots and Perturbation plot are generated by using mathematical models developed for Penetration, weld width, fusion area and UTS. These plots may be useful for prediction of the responses like UTS, penetration, width and fusion area. The response can also be estimated from these plots.
- 5) Predicted vs actual graph for UTS, penetration, Weld width and weld area, show that actual values are very close to the predicted values.
- 6) ANOVA shows that weld speed is the most significant factor, followed by current and gas flow rate. Penetration is highly influenced by weld speed and very little weld torch angle, current and weld speed have nearly same influence on weld width. Torch angle has more influence on weld width as compared to penetration.
- 7) Increase in micro hardness of weld joint is less as compared to conventional arc welding.

#### REFERENCES

- [1] Ahmed Khalid Hussain, Abdul Lateef, Mohd Javed, Pramesh.T., (2010) Influence of Welding Speed on Tensile Strength of Welded Joint in TIG welding process International Journal Of Applied Engineering Research, Dindigul Volume 1, No 3, 2010
- [2] Ahmet Durgutlu (2004) Experimental investigation of the effect of hydrogen in argon as a shielding gas on TIG welding of stainless steel Materials and Design Science Direct 25(2004)19–23
- [3] Akbari Mousavi, S. A. A., & Miresmaeili, R. (2008). Experimental and numerical analyses of residual stress distributions in TIG welding process for 304L stainless steel. *Journal of Materials Processing Technology*, 208(1), 383-394.
- [4] Arun Narayanan, Cijo Mathew, Vinod Yeldo Baby, Joby Joseph (2013) International Journal of Engineering Science and Innovative Technology (IJESIT) Volume 2, Issue 5, September 2013
- [5] Dinesh Kumar.R Elangovan.S, Siva Shanmugam.N (2014) Parametric Optimisation Of Pulsed – Tig Welding Process In Butt Joining Of 304 Austenitic Stainless Steel Sheets IJRET: International Journal of Research in Engineering and Technology eISSN: 2319-1163 | pISSN: 2321-7308
- [6] Dongjie Li, Shanping Lu Wenchao Dong, Dianzhong Li, Yiyi Li (2012) Study of the law between the weld pool shape variations with the welding parameters under two TIG processes *Journal of Materials Processing Technology* 212 (2012) 128–136
- [7] Indira Rani, M., & Marpu, R. N. (2012). Effect of Pulsed Current Tig Welding Parameters on Mechanical Properties of J-Joint Strength of Aa6351. *The International Journal of Engineering And Science (IJES)*, 1(1), 1-5.
- [8] Jyoti Prakash S.P.Tewari, Bipin Kumar Srivastava (2010) Shielding Gas for Welding of Aluminium Alloys by TIG/MIG Welding-A Review International Journal of Modern Engineering Research (IJMER) Vol.1, Issue.2, pp-690-699
- [9] Karunakaran, N. (2012). Effect of Pulsed Current on Temperature Distribution, Weld Bead Profiles and Characteristics of GTA Welded Stainless Steel Joints. *International Journal of Engineering and Technology*, 2(12)
- [10] Kumar, A., & Sundarajan, S. (2009). Optimization of pulsed TIG welding process parameters on mechanical properties of AA 5456 Aluminum alloy weldments. *Materials & Design*, 30(4), 1288-1297.
- [11] Kundan Kumar, Somnath Chattopadhyaya, Avadhesh Yadav (2012) Surface Response Methodology For Predicting The Output Responses of Tig Welding Process AJER Vol. I ISSN-2319-2100
- [12] Lothongkum, G., Viyanit, E., & Bhandhubanyong, P. (2001). Study on the effects of pulsed TIG welding parameters on delta-ferrite content, shape factor and bead quality in orbital welding of AISI 316L stainless steel plate. *Journal of Materials Processing Technology*, 110(2), 233-238
- [13] Lu, S. P., Qin, M. P., & Dong, W. C. (2013). Highly efficient TIG welding of Cr13Ni5Mo martensitic stainless steel. *Journal of Materials Processing Technology*, 213(2), 229-237
- [14] Mukesh, Sanjeev Sharma (2013) Effect of Parameters on Weld Pool Geometry in 202 Stainless Steel Welded Joint Using Tungsten Inert Gas (TIG) Process International Journal of Science and Modern Engineering (IJISME) ISSN: Volume-1, Issue-12, November 2013
- [15] Naitik S Patel, Prof. Rahul B Patel (2014) International Journal of Computational Engineering Research | Vol, 04 | Issue, 1 |
- [16] Narang, H. K., Singh, U. P., Mahapatra, M. M., & Jha, P. K. (2011). Prediction of the weld pool geometry of TIG arc welding by using fuzzy logic controller. *International Journal of Engineering, Science and Technology*, 3(9), 77-85.
- [17] Norman, A. F., Drazhner, V., & Prangnell, P. B. (1999). Effect of welding parameters on the solidification microstructure of autogenous TIG welds in an Al–Cu–Mg–Mn alloy. *Materials Science and Engineering: A*, 259(1), 53-64.
- [18] Qinglei, J., Yajiang, L., Puchkov, U. A., Juan, W., & Chunzhi, X. (2010). Microstructure characteristics in TIG welded joint of Mo–Cu composite and 18-8 stainless steel. *International Journal of Refractory Metals and Hard Materials*, 28(3), 429-433
- [19] Raveendra, A., & Kumar, B. R. (2013). Experimental study on Pulsed and Non-Pulsed Current TIG Welding of Stainless Steel sheet (SS304). *International Journal of Innovative Research in Science, Engineering and Technology*, 2(6)
- [20] Roshan W. Tulankar Suraj S. Dehankar (2013) International Journal of Engineering Trends and Technology (IJETT) - Volume 4 Issue 7- July 2013
- [21] Sakthivel, T., Vasudevan, M., Laha, K., Parameswaran, P., Chandravathi, K. S., Mathew, M. D., & Bhaduri, A. K. (2011). Comparison of creep rupture behaviour of type 316L (N) austenitic stainless steel joints welded by TIG and activated TIG welding processes. *Materials Science and Engineering: A*, 528(22), 6971-6980.
- [22] Sanjeev kumar (2010) Experimental Investigations On Pulsed Tig Welding Of Aluminium Plate IJAET/Vol.I/ Issue II/July-Sept., 2010/200-211

- [23] Sivaprasad, K., & Raman, S. (2007). Influence of magnetic arc oscillation and current pulsing on fatigue behavior of alloy 718 TIG weldments. *Materials Science and Engineering: A*, 448(1), 120-127.
- [24] Song, J. L., Lin, S. B., Yang, C. L., & Fan, C. L. (2009). Effects of Si additions on intermetallic compound layer of aluminum–steel TIG welding–brazing joint. *Journal of Alloys and Compounds*, 488(1), 217-222
- [25] Tetsumi Yuri Ogata, T., Saito, M., & Hirayama, Y. (2000). Effect of welding structure and  $\delta$ - ferrite on fatigue properties for TIG welded austenitic stainless steels at cryogenic temperatures. *Cryogenics*, 40, 251-259
- [26] Tseng, K. H., & Hsu, C. Y. (2011). Performance of activated TIG process in austenitic stainless steel welds. *Journal of Materials Processing Technology*, 211(3), 503-512
- [27] Urena, A., Escalera, M. D., & Gil, L. (2000). Influence of interface reactions on fracture mechanisms in TIG arc-welded aluminum matrix composites. *Composites Science and Technology*, 60(4), 613-622
- [28] Wang, Q., Sun, D. L., Na, Y., Zhou, Y., Han, X. L., & Wang, J. (2011). Effects of TIG Welding Parameters on Morphology and Mechanical Properties of Welded Joint of Ni-base Superalloy. *Procedia Engineering*, 10, 37-41.
- [29] Wang Rui, W., Zhenxin, L., & Jianxun, Z. (2008). Experimental Investigation on Out-of-Plane Distortion of Aluminum Alloy 5A12 in TIG Welding. *Rare Metal Materials and Engineering*, 37(7), 1264-1268
- [30] Wang Xi-he, W., Ji-tai, N., Shao-kang, G., Le-jun, W., & Dong-feng, C. (2009). Investigation on TIG welding of SiCp-reinforced aluminum–matrix composite using mixed shielding gas and Al–Si filler. *Materials Science and Engineering: A*, 499(1), 106-110.
- [31] A text book on “Welding Science and Technology”, by M.I. Khan, New age International Publishers, New Delhi, (2007).